Journal of the Korean Nuclear Society
Volume 28, Number 1, February 1996

《Technical Report》

Assessment of Gas Generation in Underground Repository of Low-Level Waste

Chan Hee Cho, Chang Lak Kim, Myung Chan Lee, and Heui Joo Choi
Korea Atomic Energy Research Institute

P.J. Agg
AEA Technology
(Received August 29, 1995)

저준위 방사성폐기물 처분장에서의 기체 발생 평가

조찬희 · 김창락 · 이명찬 · 최희주
한국원자력연구소

P.J. Agg
AEA Technology
(1995. 8. 29 접수)

Abstract

In a repository containing low-level waste, gas generation will occur principally by the coupled processes of metal corrosion and microbial degradation of cellulosic waste. This paper describes a mathematical model designed to address gas generation by these mechanisms and assesses the potential effects of gas generation on the performance of a radioactive waste repository. The metal corrosion model incorporates a three-stage process encompassing aerobic and anaerobic corrosion regimes; the microbial degradation model simulates the activities of eight different microbial populations, which are maintained as functions both of pH and of the concentrations of particular chemical species. A prediction is made for gas concentrations and generation rates over an assessment period of ten thousand years in a radioactive waste repository. The results suggest that H_2 will be the principal gas generated within the radioactive waste cavern.

요 약

방사성폐기물 처분후 처분장내에서는 금속의 부식과 셀룰로스 물질의 미생물 분해에 의한 기체가 발생하게 된다. 이 논문에서는 금속부식과 미생물 분해에 의해 발생되는 기체의 발생률을 예측하는 수학적 모델을 검토하고, 그로부터 저준위 방사성폐기물 처분장에 대한 기체 발생률을 예측하여 보았다. 금속성 물질의 부식은 3단계로 일어나며 그중 마지막 단계에서 H_2가 발생하게 된다. 셀룰로스 물질의 미생물 분해는 8가지 형태의 박테리아에 의해 일어나는 화학반응에 따라 H_2, CO_2, CH_4 등이 발생하게 되는데 이

는 처분장내의 pH 및 몇몇 화학종의 농도에 따라 반응률이 결정되게 된다. 이 논문에서는 처분후 약 10,000년 동안 발생되는 주요 기체의 발생률 및 누적발생량을 예측하여 보았다. 평가 결과, 중저준위 방사성폐기물 처분장내에서 발생되는 기체는 H_2가 가장 많이 발생되는 것을 알 수 있었다.

1. Introduction

In assessing the safety of a repository for low-level waste(LLW) in a geological structure, important issues to be considered are the generation of gas within the repository and the potential impact of such gas generation on the transport of radioactivity to the biosphere. This paper describes how the volumes and generation rates of gases within the repository may be reliably predicted over tens of thousands years that are of interest in the assessment of post-closure radiological safety.

In order to assess the implications of gas generation for the safety of a deep repository for LLW, it is important to gain an understanding of the principal mechanisms of gas generation. This understanding can then be used to assist in the prediction of the likely cumulative volumes of gas generated within the repository, and of the variation of the rate of gas generation with time. Given an understanding of the physical and chemical properties of the repository and host rock, the predicted gas generation rates can be used to determine whether there is likely to be a pressure build-up within the repository environment, or whether gas will migrate out of the repository easily.

The dominant source of gas generation within a repository is likely to be anaerobic corrosion of metals, resulting in evolution of H_2. The principal source of microbiological gas generation in LLW is expected to be the degradation of cellulosic wastes such as wood, cardboard, paper and tissues. The principal gases generated by this process are CO_2 and CH_4 although small amounts of H_2, N_2 and H_2S will also be generated. The assessment of gas generation in this study is carried out for LLW repository using the GAMMON program[1, 2] developed by AEA Technology of the UK.

2. Model Description

2.1. Metal Corrosion Model

The dominant source of gas generation within a repository is likely to be anaerobic corrosion of metals, resulting in the evolution of hydrogen. The principal metal within a radioactive waste repository will be steel, either as waste or as associated packaging. As iron is the major component of steel, it is the corrosion of iron that is assumed to be the major contributor to gas generation by this mechanism, and this is incorporated in the model. Because the repository environment will initially be aerobic, corrosion is considered to proceed by means of three-stage process encompassing both the aerobic and anaerobic regimes. The various possible reactions in the three stages are given in Fig. 1.

The first stage involves the corrosion of iron metal. When oxygen is used up, the oxide film on the iron metal is reduced to Fe_3O_4(magnetite) under anaerobic environment. In the second stage, magnetite is assumed to be formed clear of the metal surface, thus exposing bare iron metal and allowing the third stage, that of anaerobic corrosion, to occur.

Two independent models are employed, both based on this chemical process, but exploiting the differences in geometry between plates and spheres. This allows differentiation of metal packaging(modelled as

(a) oxidation('rusting') of iron:

$$4Fe + 3O_2 \rightarrow 2Fe_2O_3$$

(b) after O_2 is depleted, oxide-film reduction:

$$4Fe_2O_3 + Fe \rightarrow 3Fe_3O_4$$

(c) anaerobic corrosion of iron:

$$3Fe + 4H_2O \rightarrow Fe_3O_4 + 4H_2$$

Fig. 1. Chemical Reactions in the Metal Corrosion Process

thin plates) and bulk waste(modelled, in general, as spheres). For any initial quantity of metal, plates and spheres represent the two extremes with regard to rate of loss of metal, and thus the two models cover the likely limits of gas generation. There are also independent models for mild and stainless steel as the corrosion rates of these two types of steel are different.

2.2. Microbial degradation model

The principal source of microbiological gas generation in LLW is expected to be the degradation of cellulosic wastes such as wood, cardboard, paper, and tissues. Although in reality this degradation is likely to be mediated by several different microbial populations[2], it is most convenient to describe the degradation by a series of representative chemical reactions mediated by eight different microbes[1]. This series of reactions is given in Fig. 2.

Initially, the model simulates the physical degradation of bulk cellulose to soluble cellulose or polysaccharide, followed by the hydrolysis of this soluble

(a) Physical degradation of bulk cellulose

Bulk cellulose → Soluble cellulose/polysaccharide

(b) Hydrolysis of soluble cellulose/polysaccharide

$[C_6H_{10}O_5]_n + nH_2O \rightarrow nC_6H_{12}O_6$

(c) Further microbially-mediated degradation

(i) aerobic degradation of organic material (Microbe type 1)

$C_6H_{12}O_6 + 6O_2 \rightarrow 6CO_2 + 6H_2O$

(ii) nitrate reduction (Microbe type 2)

$C_6H_{12}O_6 + 4.8HNO_3 \rightarrow 6CO_2 + 2.4N_2 + 8.4H_2O$

(iii) anaerobic acidogenesis (Microbe type 3)

$C_6H_{12}O_6 + H_2O \rightarrow 2CO_2 + 2H_2 + C_2H_5OH + CH_3COOH$

(iv) anaerobic acetogenesis (Microbe type 4)

$C_2H_5OH + H_2O \rightarrow CH_3COOH + 2H_2$

(v) acetoclastic methanogenesis (Microbe type 5)

$CH_3COOH \rightarrow CO_2 + CH_4$

(vi) hydrogen-utilizing methanogenesis (Microbe type 6)

$CO_2 + 4H_2 \rightarrow CH_4 + 2H_2O$

(vii) acetoclastic sulphate reduction (Microbe type 7)

$CH_3COOH + H_2SO_4 \rightarrow H_2S + 2CO_2 + 2H_2O$

(viii) hydrogen-utilizing sulphate reduction (Microbe type 8)

$4H_2 + H_2SO_4 \rightarrow H_2S + 4H_2O$

Fig. 2. Chemical Reactions in the Microbial Degradation Model

form to a glucose-type monomer. This hydrolysis is likely to occur both naturally and by microbial mediation[3], and the relative rates of these two processes are determined by the pH of the repository environment. The resulting glucose-type monomer then acts as the initial substrate for further degradation mediated by eight different microbial populations, as shown in Fig. 2. The microbial populations are themselves maintained at levels that are dependent on the pH of the repository environment, as well as on the availability of metabolic nitrogen(NH_4^+), water and particular substrates or inhibitors.

This degradation scheme encompasses both aerobic and anaerobic regimes. While the repository environment is aerobic, the dominant microbially-mediated reaction is the aerobic decomposition of the glucose-type monomer by microbe type 1. Once the environment has become sufficiently anaerobic, the other microbial populations begin to grow. These populations consist of nitrate reducers(microbe type 2), acidogens(microbe type 3), acetogens (microbe type 4), methanogens(microbe types 5 and 6) and sulphate reducers(microbe types 7 and 8).

Acidogenesis of the glucose-type monomer is mediated by microbe type 3, resulting in the formation of intermediate organic acids, with the liberation of carbon dioxide and hydrogen. Microbe type 4 mediates the acetogenesis reaction in which the intermediate acids(represented conveniently in the model by ethanol) are hydrolysed to acetate. If there are substantial quantities of nitrate and sulphate ions available, either in the groundwater or within the waste, the nitrate- and sulphate-reducing microbial populations (microbe types 2, 7 and 8) will grow in preference to the methanogens(microbe types 5 and 6), generating nitrogen and hydrogen sulphide as product gases. Once all of the nitrate and sulphate ions have been consumed, microbe types 5 and 6 will begin to grow more rapidly and a fully anaerobic methanogenic regime will become established.

2.3. Model Reaction Rates

The chemical reactions in the metal corrosion model and the microbial degradation model are governed by suitable rate equations. For example, in the microbial degradation model the rate of change of concentration of a particular microbial population, m, is given by

$$\frac{dm}{dt} = Gm - Dm, \tag{1}$$

where G is the growth rate and D the death rate of the population. The growth and death rates are both conditioned by the chemical environment. The chemical conditioning of the growth rate is effectively modelled using the Monod equation[3]. For example, if an aerobic microbial population is being considered (e. g. microbe type 1), then the growth rate is modified so that

$$G = \mu \frac{[O_2]}{[O_2] + K_s} \tag{2}$$

where μ is a constant growth rate that applies under optimal conditions, $[O_2]$ is the concentration of oxygen and K_s is a constant saturation coefficient. If there is a significant concentration of oxygen in the system, the fraction $[O_2]/([O_2]+K_s)$ is approximately unity and the growth rate is not significantly altered. On the other hand, if the concentration of oxygen is low, that is the system is almost anaerobic, the fraction tends to be zero and the growth rate is greatly reduced.

The growth rate for an anaerobic microbial population is conversely given by

$$G = \mu \left[1 - \frac{[O_2]}{[O_2] + K_i} \right] \tag{3}$$

where K_i is an inhibition coefficient. In this case, if there is a significant concentration of oxygen in the system, the quantity $(1-[O_2]/[O_2]+K_i))$ tends to be zero and the growth rate is greatly reduced. On the other hand, if the concentration of oxygen is low, the same quantity is approximately unity, and the growth rate is not significantly altered.

The modelling of the chemical conditioning is achieved by the use of such saturation and inhibition terms for each of the microbes. Monod kinetics have been applied extensively for dynamic modelling systems such as this. The application of Monod kinetics to a dynamic system assumes that sequential reactions of digestion can be represented by calculating population growth rates and mass balances over each step independently. The equation is empirically based and has been used extensively for dynamic modelling work requiring a computer solution[4, 5, 6, 7]. The model therefore comprises a set of coupled first-order differential equations, one for each component of the system. The values of the rate constants governing some of the equations differ by several orders of magnitude, and as a result the system is numerically somewhat stiff. The equations are solved in the GAMMON program using an appropriate routine[8]. The variations of each component of the system are thus evaluated with respect to time.

Three chemical components of the system(oxygen, water and hydrogen) are common to both the metal corrosion and the microbial degradation models, and this results in the coupling of the two models. For example, in the aerobic phase the utilization of oxygen by microbe type 1 is competitive with the aerobic corrosion of iron to produce Fe_2O_3. Both models are also dependent on the pH of the repository environment. The growth rates of the various microbial populations are modified according to a pH dependence function built into GAMMON, and different metal corrosion rates are used for high and neutral pH repository environments[9]. The formation of organic acids in the microbial degradation process will result in a reduction of pH, and this may in turn affect the local metal corrosion rate. However, this effect is neglected in the corrosion model.

The GAMMON program is based on a mathematical model in which gas generation is modelled by the coupled processes of metal corrosion and mi-

crobial degradation of cellulose. For both gas generation processes, the mathematical model is based on a set of chemical reactions that are representative of the likely reactions under this range of conditions, and that cover the dominant gas-generating mechanisms. GAMMON can be used to estimate the quantity, composition and generation rate of gas over the timescales of interest in operational and post-closure safety assessments.

A series of validation experiments using small scale columns and full size 200 liter drums have been undertaken for the GAMMON program[1]. Twelve drums were filled with mixed LLW simulant material under a variety of moisture and pH environments. They were then buried underground and the gas composition and generation rates were monitored continuously over a three-year period[10]. There is generally good agreement between the experimental and predicted gas concentrations. More comprehensive model validation program is being proceeded by the UK Nirex[11].

3. Repository Design Used for Evaluation of Gas Generation Rates

The repository design considered here consists of the following five caverns[12] :

(a) LLW(Type I) cavern;
(b) LLW(Type II) caverns(two caverns);
(c) LLW(Type III) cavern;
(d) LLW(Type IV) cavern.

A summary information for each cavern associated with each waste type, and of the total volume occupied by the waste form, is provided in Table 1. Also dimensions of each cavern are given in Table 2. Only the LLW(Type Ⅳ) cavern containing higher radioactivity than other caverns is assumed to be backfilled

Table 1. Waste Inventory for Each Cavern

Waste type	Number of drums				
	LLW (Type I)	LLW (Type Ⅱ)	LLW (Type Ⅲ)	LLW (Type Ⅳ)	Volume occupied (m^3)
Liquid conc. in cement	10,425	–	4,996	–	3.08×10^3
Liquid conc. in paraffin	–	–	–	10,273	2.05×10^3
Ion exchange resin in cement	4,516	–	–	–	9.03×10^2
Ion exchange resin in HIC	–	–	–	16,445	3.29×10^3
Spent filters in cement	4,307	–	–	882	1.04×10^3
General trash	–	36,288	11,868	–	9.63×10^3

Table 2. Dimensions for Each Cavern

	LLW I	LLW Ⅱ	LLW Ⅲ	LLW Ⅳ
Dimension(m) (w)×(h)×(l)	18.6×10.5×140	20.6×10.5×140	20.6×10.5×140	19.1×21.0×140

in this preliminary design concept.

In order to provide an estimate of the likely cumulative amounts and generation rates of bulk gases within the imaginary repository, the GAMMON program is applied in this assessment. Three independent source terms are considered in these calculations :

(a) LLW(Type I) cavern ;
(b) LLW(Type II/III) caverns - 2 Type II caverns, 1 Type III cavern ;
(c) LLW(Type IV) cavern.

These three source terms were selected on the basis of the backfilling strategies for the various caverns. Given these various backfilling strategies, the key parameter affecting gas generation is likely to be the pH of the repository porewater. This parameter has a significant effect both on the rate of anaerobic metal corrosion and on the rate of microbial degradation of cellulosic wastes. A series of calculations is performed in this assessment as follows :

(a) Case 'LLW1A' : LLW(Type I) cavern-pH12(variable) ;
(b) Case 'LLW1B' : LLW(Type I) cavern-pH7(variable) ;
(c) Case 'LLW2/3A' : LLW(Type II/III) caverns-pH7 (variable) ;
(d) Case 'LLW2/3B' : LLW(Type II/III) caverns-pH7 (buffered) ;
(e) Case 'LLW4A' : LLW(Type IV) cavern-pH12(variable) ;
(f) Case 'LLW4B' : LLW(Type IV) cavern-pH12(buffered) ;
(g) Case 'LLW4C' : LLW(Type IV) cavern-pH9(variable) ;
(h) Case 'LLW4D' : LLW(Type IV) cavern-pH7(variable).

For the purpose of this illustrative assessment, it is assumed that the repository environment is completely anaerobic at the time of closure of the caverns. Although there may be some delay in achieving anaerobic conditions because of the existence of significant amounts of oxygen in the caverns at the time of closure, the assumption made here leads to conservative estimates of gas generation rates within the repository, particularly in the early post-closure period. Major input data used in these caculations are given in Table 3.

In Table 3, initial concentration of mild steel(plate), C_{mp}, is derived from

$$C_{mp} = n_d m_d / V_c \tag{4}$$

where n_d is number of mild steel drums in cavern, m_d is mass of mild steel 200 liter drum, V_c is cavern volume. Initial concentration of mild steel(sphere), C_{ms}, is derived from

$$C_{ms} = n_d f_m m_w / V_c \tag{5}$$

where f_m is fraction of trash weight that is metal(approximately 20%) and m_w is average mass of all waste in one drum(112kg). Similarly, initial concentration of stainless steel(plate), C_{sp}, is given by

$$C_{sp} = n_h m_h / V_c \tag{6}$$

where n_h is number of stainless steel HICs in cavern and m_h is mass of stainless steel HICs. Also, initial concentration of bulk cellulose, C_{ce}, is derived from

$$C_{ce} = n_c f_c m_w / V_c \tag{7}$$

where n_c is number of cellulose-containing drums (spent filter drums in LLW(Type I) and LLW(Type IV) caverns, all drums in LLW(Type II/III) caverns), and f_c is fraction of waste that is cellulosic (assumed to be 1% in spent filter drums and 29% in trash drums).

In this study, initial concentrations of SO_4^{2-} and NO_3^- in wastes are assumed to be zero due to data limitation. However, for cation spent resin drums, this assumption may not be adequate.

Table 3. Major Input Data Used in the GAMMON Calculations

Parameter	LLW(Type I) cavern	LLW(Type II / III) caverns	LLW(Type IV) cavern
vault volume(m^3)	2.73×10^4	9.09×10^4	5.62×10^4
initial concentrations(kg/m^3) of			
mild steel (plate)	17.6	54.4	4.96
mild steel (sphere)	–	11.9	–
stainless steel (plate)	–	–	58.2
bulk cellulose	1.77×10^{-1}	17.2	1.76×10^{-2}
H_2O (in waste)	3.95	3.27	2.75
NH_4^+ (in waste)	7.08×10^{-4}	6.88×10^{-2}	7.04×10^{-5}
NO_3^- (in waste)	–	–	–
SO_4^{2-} (in waste)	–	–	–
initial plate thickness(m) of			
mild steel	1.20×10^{-3}	1.20×10^{-3}	1.20×10^{-3}
stainless steel	–	–	1.00×10^{-2}
initial sphere radius of mild steel(m)	–	1.00×10^{-2}	–
$^{14}C/^{12}C$ ratio	2.53×10^{-9}	6.14×10^{-10}	5.84×10^{-6}
^3H release rate from mild steel (Bq/m^3yr)	–	2.44×10^2 (for 1110 yrs)	–
concentrations in groundwater(kg/m^3) :			
SO_4^{2-}	9.98×10^{-3}	9.98×10^{-3}	9.98×10^{-3}
NO_3^-	–	–	–
vault resaturation rate(m^3/m^3hr)	4.11×10^{-5}	4.33×10^{-5}	1.37×10^{-5}
groundwater flow rate through vault (m^3/m^3hr)	2.79×10^{-6}	2.94×10^{-6}	2.23×10^{-9}
resaturation H_2O concentration(kg/m^3)	9.00×10^2	9.50×10^2	3.00×10^2

4. Results and Discussions

4.1. LLW(Type I) cavern

The results in Tables 4 to 6 and Figs. 3 and 4 suggest that H_2 will be principal gas generated within the LLW(Type I) cavern, with $4.1\times10^2 mol/m^3$ of H_2 generated over the lifetime of the repository. In the case that alkaline conditions prevail within the waste packages(Case LLW1A), metal surfaces will be predominantly corroded by high-pH groundwater, and the peak generation rate of H_2 ($3.7\times10^{-1}mol/m^3yr$) is therefore likely to be about one order of magnitude less than if the corroding groundwater is not conditioned to a high pH by the cementitious grout(Case LLW1B). Although the maximum generation rate is lower in Case LLW1A, H_2 is generated at this rate for a longer period of time(possibly up to a few thousand years after closure). By comparison, relatively small quantities of CO_2 and CH_4 will be generated within this cavern; this is a consequence of the small amount of cellulosic material assumed to be present within the waste(see Table 3). In the case that alkaline conditions prevail within the packages (Case LLW1A), although the cumulative amount of carbon gases generated is predicted to be some two orders of magnitude less than that of H_2, the peak generation rate of these gases could be comparable to (or possible greater than) the maximum generation rate of H_2.

The peak generation rates of the microbially generated gases predicted by GAMMON tend to be rela-

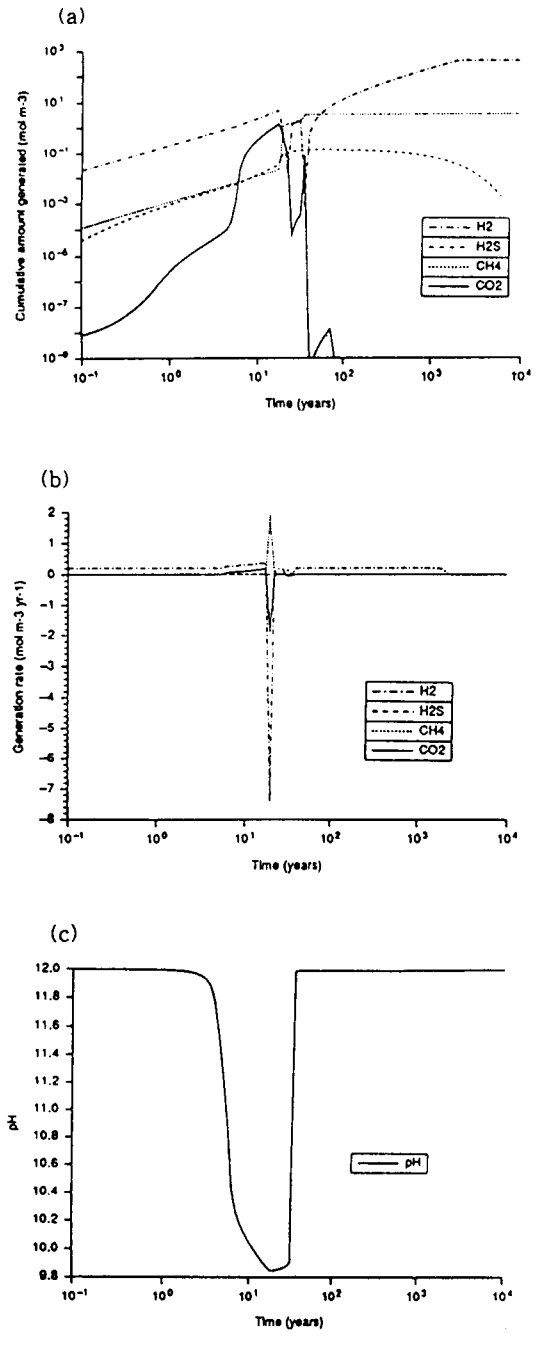

Fig. 3. (a) Cumulative amounts generated, (b) generation rates of gases and (c) variation of pH as functions of time within LLW(Type I) cavern : initial pH 12 (variable)

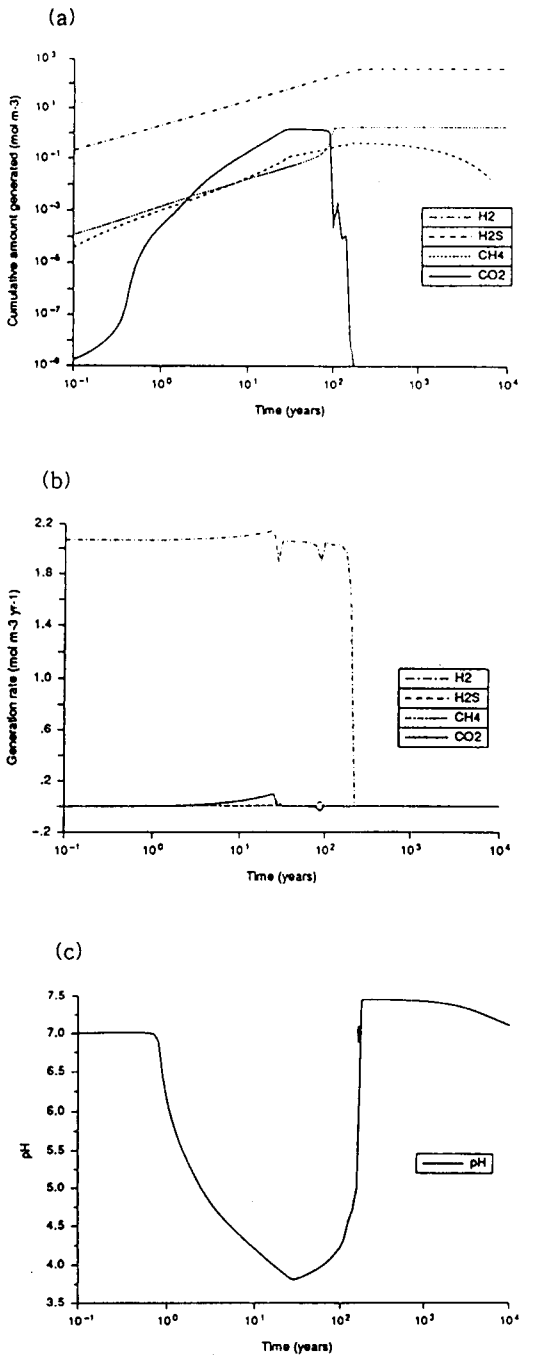

Fig. 4. (a) Cumulative amounts generated, (b) generation rates of gases and (c) variation of pH as functions of time within LLW(Type I) cavern : initial pH 7 (variable)

tively short-lived; this is a result of modelling the cavern as a homogeneous mixture, in which environmental conditions are assumed to be uniform throughout the cavern. In reality, the cavern environment will be quite heterogeneous, and microbial growth will probably occur at different rates within different regions of the cavern. As a consequence, the peaks in the generation rates of CO_2 and CH_4 will tend to be both broader and lower.

In Figs. 3(c) and 4(c), the predicted variation of pH as a function of time is illustrated graphically. In the case that the groundwaters are conditioned by the grout to a high pH(Fig. 3(c)), the pH is not expected to be fall much below 10.0. In the case that poor conditioning occurs(Fig. 4(c)), however, the pH could be reduced to 4.0 as a result of the build-up of organic acids resulting from microbial degradation of cellulose; this has the effect of delaying the onset of methanogenesis, as illustrated by the results in Table 6.

4.2. LLW(Type II/III) Caverns

The results in Tables 4 to 6 and Figs. 5 and 6 suggest that H_2 is likely to be the principal gas generated within the LLW(Type Ⅱ/Ⅲ) caverns, although the amounts of CO_2 and CH_4 generated are likely to be considerably greater than in Type I cavern. This is a result of the high cellulosic content of the trash wasteforms in the Type Ⅱ/Ⅲ caverns, compared with that of the spent filters in the Type I cavern. The predicted total cumulative amount of H_2 generated in the Type Ⅱ/Ⅲ caverns (approximately $10^3 mol/m^3$) is greater that generated in the Type I cavern by a factor of two or three, which is a result of the higher concentration of waste drums within these caverns, and the presence of waste metal within the trash wasteform. By comparison, the predicted total cumulative amount of CH_4 generated in the Type Ⅱ/Ⅲ caverns (approximately $2 \times 10^2 mol/m^3$) is two orders of magnitude greater than that in the Type I cavern.

It is interesting to note the difference between the predicted times of peak generation rate of CH_4 in Cases LLW2/3A and LLW2/3B (see Table 6). In the former case, in which the pH within the cavern is al-

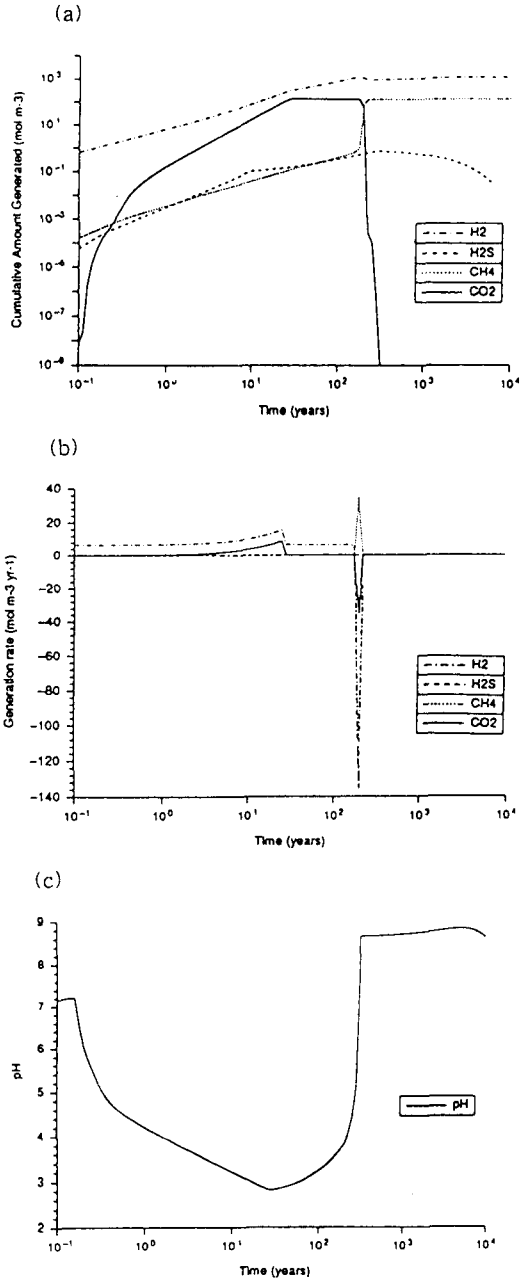

Fig. 5. (a) Cumulative amounts generated, (b) generation rates of gases and (c) variation of pH as functions of time within LLW(Type Ⅱ/Ⅲ) cavern : initial pH 7 (variable)

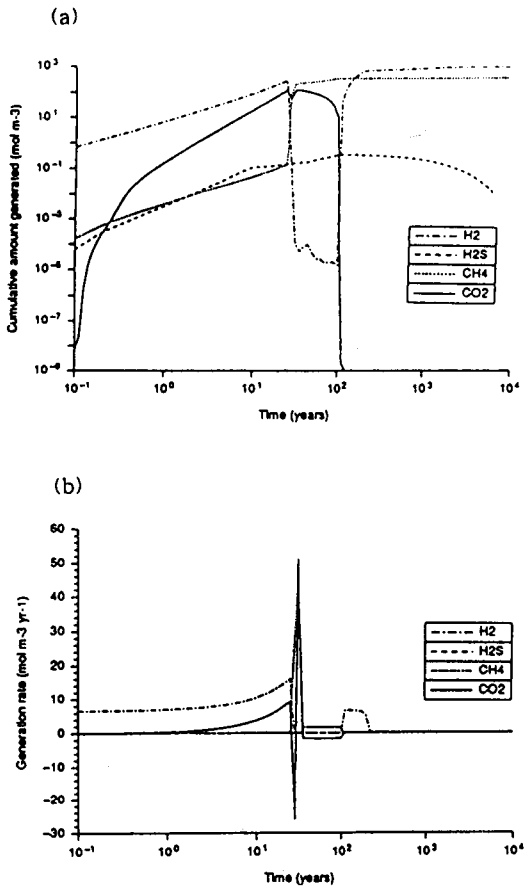

Fig. 6. (a) Cumulative amounts generated and (b) generation rates of gases as functions of time within LLW(Type Ⅱ/Ⅲ) cavern : initial pH 7 (buffered)

lowed to vary as a function of time, the peak generation rate of CH_4 is predicted to be delayed until some 200 years after repository closure, whereas in the latter case, in which the pH is fixed at 7, the peak rate is predicted to occur after only 30 years. This is explained by the significant reduction in pH within the caverns as a result of the build-up of organic acids resulting from microbial degradation of cellulosic materials (see Fig. 5(c)).

4.3. LLW(Type IV) cavern

In the case of the LLW(Type Ⅳ) cavern, four GAMMON calculations are undertaken : two in which a cementitious backfill is assumed(Cases LLW4A and LLW4B) ; one in which a bentonite/crushed rock backfill is assumed ; one in which no backfill is assumed (Case LLW4D). The results in Tables 4 to 6 and Figs. 7 to 10 indicate that, similarly to the LLW(Type Ⅰ) cavern, H_2 will be the principal gas generated within the LLW(Type Ⅳ) cavern, although the total cumulative amount generated (2×10^{2}mol/m^3) will be less than that in the LLW(Type Ⅰ) cavern. The cumulative amount of CH_4 generated (5.9×10^{-1}mol/m^3) is insignificant by comparison. The maximum rate of generation of H_2 will be very dependent on the backfilling strategy. The anaerobic steel corrosion rate tends to decrease with increasing pH; in these calculations, the anaerobic corrosion rate at pH 7 was assumed to be one order of magnitude greater than that at pH 12.

As a consequence, the maximum generation rate of H_2 in Cases LLW4A and LLW4B (approximately 7×10^{-2}mol/m^{3}yr) is about one order of magnitude less than that in LLW4D (5.9×10^{-1}mol/m^{3}yr), although that rate is likely to endure for a longer period of time(possibly for a few thousand years, as in Case LLW1A for the LLW(Type Ⅰ) cavern). Whichever backfill strategy is adopted, H_2 is likely to continue to be generated at a lower rate (8.2×10^{-3}mol/m^{3}yr) for several thousand years as a result of the corrosion of the stainless steel HIC drums, which is expected to occur at a lower rate than corrosion of the mild steel drums.

As noted above, the rates of generation of CO_2 and CH_4 are likely to be insignificant by comparison with H_2 ; this is because of the relatively low cellulosic content in the wasteforms. However, it is still possible that there could be a significant reduction in cavern pH resulting from the build-up of organic acids from microbial degradation of cellulosic materials. In the case of the cementitious backfill(Case LLW4B, initially pH 12), this will tend to enhance the onset of methanogenesis, whereas in the case of no backfill (Case LLW4D, initially pH 7), the effect is to delay

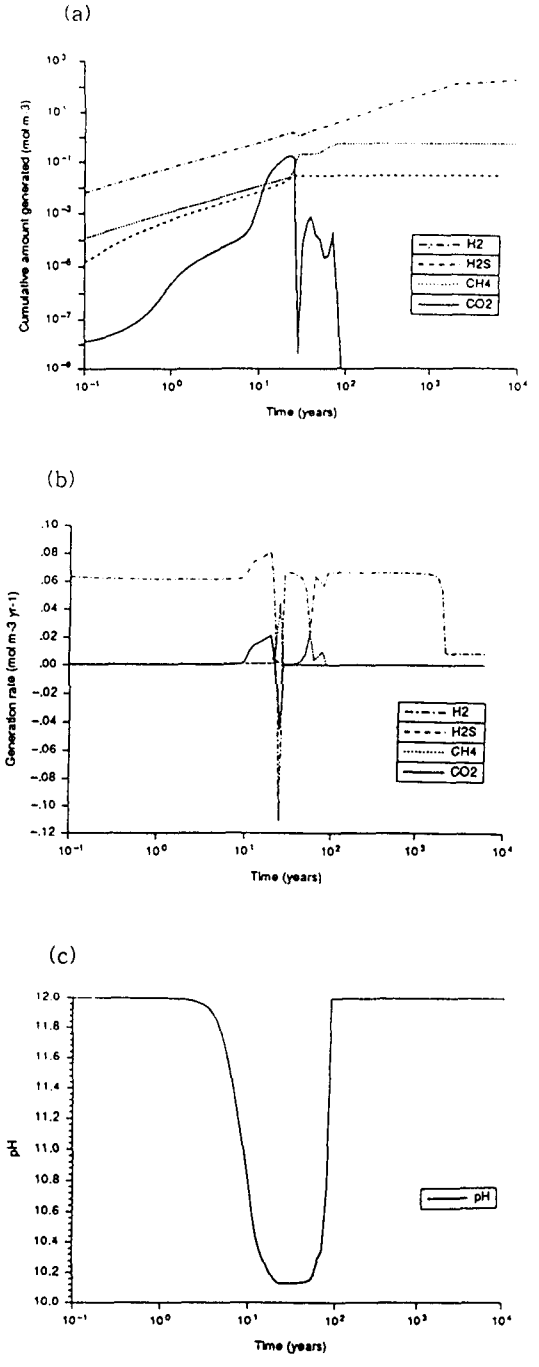

Fig. 7. (a) Cumulative amounts generated, (b) generation rates of gases and (c) variation of pH as functions of time within LLW(Type Ⅳ) cavern: initial pH 12 (variable)

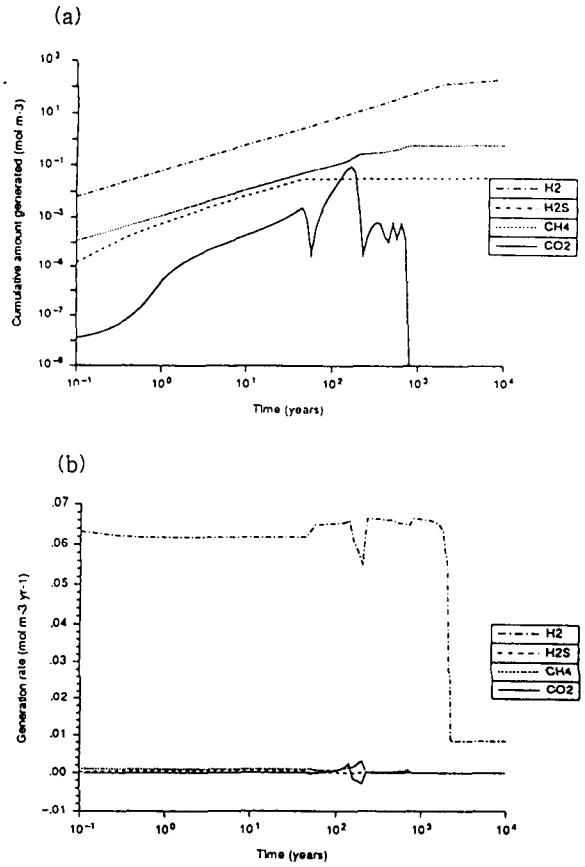

Fig. 8. (a) Cumulative amounts generated and (b) generation rates of gases as functions of time within LLW(Type Ⅳ) cavern: initial pH 12 (buffered)

the onset of methanogenesis, as in the LLW(Type Ⅱ/Ⅲ) cavern.

In interpreting such a theoretical prediction, it is important to consider the uncertainties associated with modelling gas generation on this time-scale. For example, it is likely that free gas will escape from the repository environment, or in the case of carbon dioxide, be chemisorbed onto the cementitious backfill to form calcium carbonate. This means that significant quantities of hydrogen and carbon dioxide generated early in the post-closure period will be removed from the gas generation system and thus not be available for subsequent use by methanogenic microbial populations. However, keeping such uncertain-

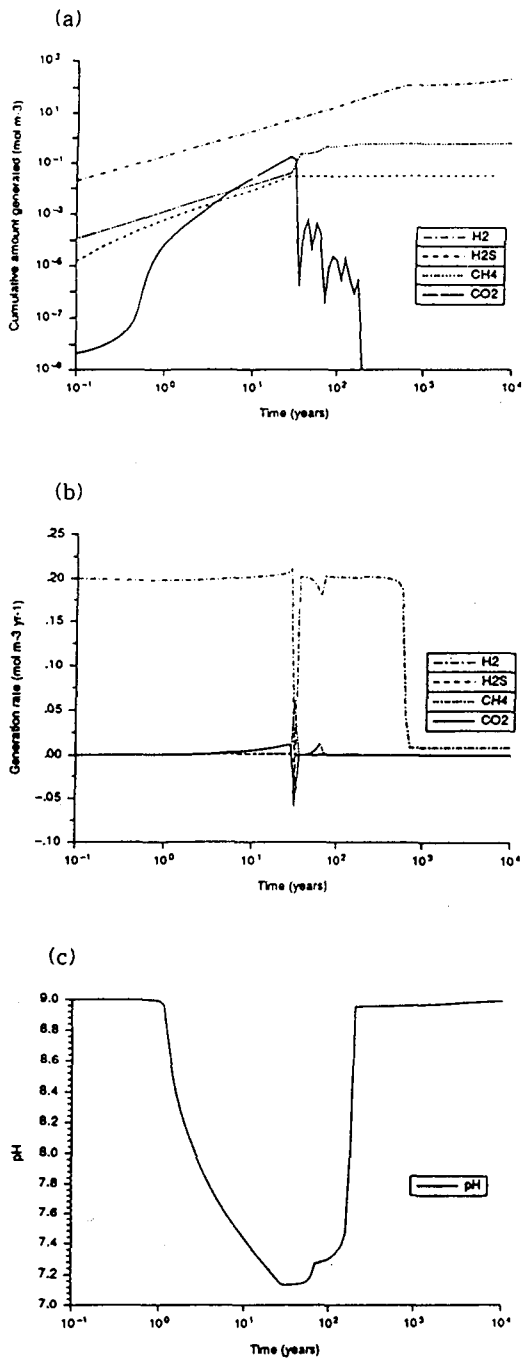

Fig. 9. (a) Cumulative amounts generated, (b) generation rates of gases and (c) variation of pH as functions of time within LLW(Type Ⅳ) cavern: initial pH 9 (variable)

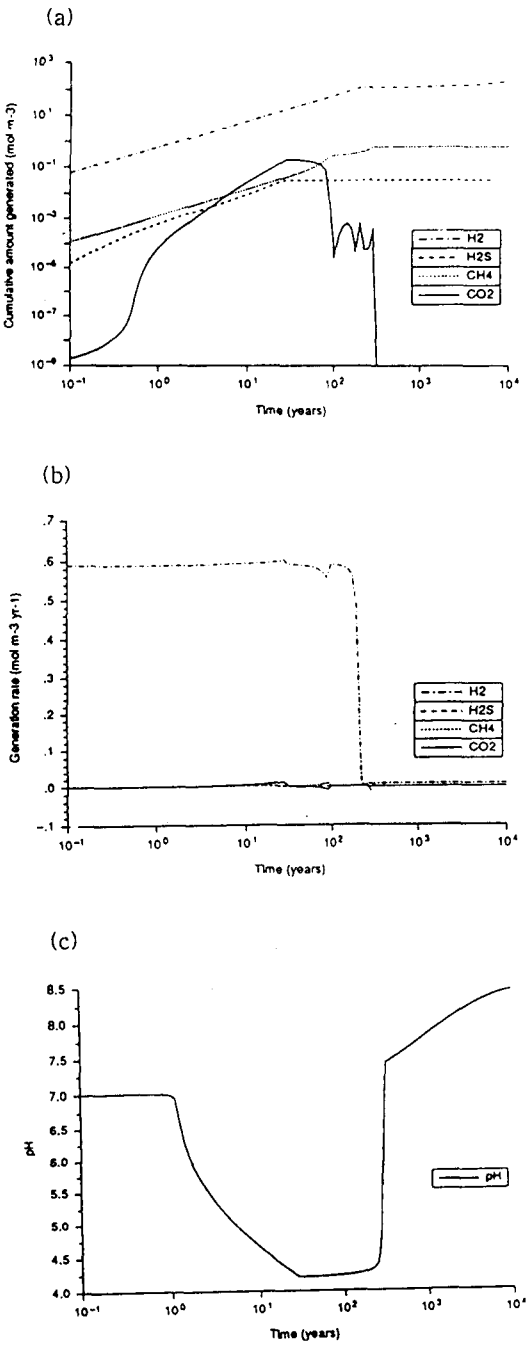

Fig. 10. (a) Cumulative amounts generated, (b) generation rates of gases and (c) variation of pH as functions of time within LLW(Type Ⅳ) cavern: initial pH 7 (variable)

Table 4. Total Cumulative Amounts Generated, Peak Generation Rates and Times of Peak for H_2

Caverns		Total Cumulative Amount Generated (mol/m^3)	Peak generation rate (mol/m^3yr)	Time of Peak (years)
LLW (Type I)	LLW1A	4.1×10^{2}	3.7×10^{-1}	18
	LLW1B	4.1×10^{2}	2.1	0−100
LLW (Type II/III)	LLW2/3A	1.2×10^{3}	16	25
	LLW2/3B	8.7×10^{2}	16	25
LLW (Type IV)	LLW4A	200	8.2×10^{-2}	20
	LLW4B	200	6.7×10^{-2}	220−790
	LLW4C	200	2.0×10^{-1}	0−500
	LLW4D	200	5.9×10^{-1}	0−130

Table 5. Peak Generation Rates and Times of Peak for CO_2

Caverns		Peak generation rate (mol/m^3yr)	Time of Peak (years)
LLW (Type I)	LLW1A	1.8×10^{-1}	18
	LLW1B	9.6×10^{-2}	25
LLW (Type II/III)	LLW2/3A	8.9	25
	LLW2/3B	48	32
LLW (Type IV)	LLW4A	2.2×10^{-2}	20
	LLW4B	2.6×10^{-3}	140
	LLW4C	1.1×10^{-2}	28
	LLW4D	1.1×10^{-2}	28

an indication of the maximum rate of gas generation that could be expected at any particular time.

In interpreting these figures, it should be remembered that the model assumes a homogeneous system, whereas in reality the repository will be heterogeneous. Switches between metal corrosion and methanogenesis will therefore occur at different times in different regions of the repository. As a consequence, the sharp peaks that are obserbed in this figure will, in reality, be both broader and lower.

Table 6. Total Cumulative Amounts Generated, Peak Generation Rates and Times of Peak for CH_4

Caverns		Total Cumulative Amount Generated (mol/m^3)	Peak generation rate (mol/m^3yr)	Time of Peak (years)
LLW (Type I)	LLW1A	3.4	1.9	20
	LLW1B	1.8	4.1×10^{-2}	89
LLW (Type II/III)	LLW2/3A	1.3×10^{2}	35	200
	LLW2/3B	3.4×10^{2}	51	32
LLW (Type IV)	LLW4A	5.9×10^{-1}	4.5×10^{-2}	25
	LLW4B	5.8×10^{-1}	3.2×10^{-3}	200
	LLW4C	5.9×10^{-1}	6.0×10^{-2}	32
	LLW4D	5.9×10^{-1}	9.9×10^{-3}	280

ties in mind, the model provides an indication of the likely volumes of gas that will be generated within the repository over the assessment period. The prediction of the variation in gas generation rates provides

5. Conclusions

This study is made for gas concentrations and gen eration rates over an assessment period of ten thou-

sand years in a radioactive waste repository using the GAMMON computer program. The results suggest that H_2 will be the principal gas generated within the radioactive waste cavern.

The maximum rate of generation of H_2 will be very dependent on the backfilling strategy. The maximum generation rate of H_2 in a cementitious backfill is about one order of magnitude less than that in a bentonite/crushed rock backfill or without backfill. The rates of generation of CO_2 and CH_4 are likely to be insignificant by comparison with H_2; this is because of the low cellulosic content in the wasteforms. The pH of the repository porewater is found to be the key parameter in the prediction of gas generation with a significant effect both on the rate of anaerobic metal corrosion and on the rate of microbial degradation of cellulosic wastes.

References

1. P.J. Agg, "Modelling Gas Generation in Radioactive Waste Repositories," *Nucl. Energy*, **32**, No. 2, pp. 81−87 (1993)
2. G. Purdom and P.J. Agg, "GAMMON(Version 1A) : A Computer Program Addressing Gas Generation in Radioactive Waste Repositories. Part A : Overview," UK Nirex Ltd Report *NSS/R338*, in preparation (1993)
3. B. Atkinson and A. Mavituna, "Biochemical Engineering and Biotechnology Handbook," Macmillan (1983).
4. D.T. Hill, "Modelling Techniques and Computer Simulation of Agricultural Waste Treatment Processes," *Agricultural Wastes*, **2**, pp. 135−156 (1980)
5. D.T. Hill and C.L. Barth, "A Dynamic Model for Simulation of Animal Waste Digestion," *J. Water Pollution Control Federation*, **49**, No. 10, pp. 2129−2143 (1977)
6. D.T. Hill, "A Comprehensive Dynamic Model for Animal Waste Methanogenesis," *Tran. Am. Soc. Agric.* Eng., 25, No. 5, pp. 1374−1380 (1982).
7. D.T. Hill, E.W. Tollner and R.D. Holmberg, "The Kinetics of Inhibition in Methane Fermentation of Swine Manure," *Agricultural Wastes*, **5**, No. 2, pp. 105−123 (1983)
8. R.G. Myhill, "DC06AD : User Documentation, Computational Fluid Dynamics Department," AEA Industrial Technology, Harwell Laboratory, UK (1991)
9. P.J. Agg *et al.* "NSARP Reference Document : Gas Generation and Migration," UK Nirex Ltd Report *NSS/G120* (1993)
10. C. McDonald et al., "Investigations into the Potential Rates, Quality and Generated Pressure of Gas Generated from the Biodegradation of Simulated LLW," UK Nirex Ltd Report *NSS/R322* (1993)
11. Y. Gunn et al., "A Critical Assessment and Approach to Validation of the Gas Generation Program GAMMON," UK Nirex Ltd Report *NSS/R299* (1994)
12. H.S. Park et al., "A Study on the Requirements for Basic Design of a Repository for Low-Level Radioactive Waste," Korea Atomic Energy Research Institute Report *KAERI-NEMAC/PR-32/93* (1993)